



Thermal degradation behaviors of sawdust wood waste: pyrolysis kinetic and mechanism

MY. Guida^{1,2,*}, S. Lanaya², Z. Rbihi², A. Hannioui^{1,2}

¹Department of Chemistry and Environment, Faculty of Sciences and Techniques (FST), University of Sultan Moulay Slimane, 23000 Béni-Mellal, Morocco.

²Organic Chemistry and Analytical Laboratory, Faculty of Sciences and Techniques (FST), University of Sultan Moulay Slimane, 23000 Béni-Mellal, Morocco.

Received 25 May 2019,
Revised 22 August 2019,
Accepted 23 August 2019

Keywords

- ✓ Sawdust wood waste
- ✓ Pyrolysis
- ✓ Thermogravimetric analysis
- ✓ Kinetic analysis parameters
- ✓ TGA-DTG

myassinaguida@gmail.com
Phone: +212523480218;
Fax: +212523481351.

Abstract

In this study, the thermal behavior of sawdust wood (SW) wastes samples was examined at different heating rates (β) ranging from 2 to 15 °C/min in inert atmosphere using the technique of thermogravimetric analysis (TGA). As the increment of heating rates, the variations of characteristic parameters from the TG-DTG curves were determined. Eight methods: Friedman (FR), Ozawa-Flynn-Wall (OFW), Vyazovkin (VYA), Kissinger-Akahira-Sunose (KAS), Starink method (ST), Avrami theory (AT), Coats-Redfern and Criado methods were used in this work to evaluate the kinetic parameters, including apparent activation energy (E_x), reaction order (n) and the appropriate conversion model $f(x)$. For the range of conversion degree (x) investigated (20 – 80 %), the mean values of apparent activation energy for Sawdust wood waste were 168 KJ/mol, 153 KJ/mol and 164 KJ/mol for FR, OFW and VYA methods respectively. While for KAS and ST methods were 158 KJ/mol and 156 KJ/mol. With varied temperature (300-700 °C), the corresponding values of reaction order (n) was increased from 0.1072 to 0.2587, along with a decrease to 0.1635. The pyrolysis model $f(x)$ of SW is described by reaction order (F_n), first order (F_1) for the degradation of the studied wastes samples.

1. Introduction

In the view of the shortage of fossil fuels and with the increasing concerns regarding human impacts on the environment, renewable energy sources and waste materials play an important role as a viable alternative to fossil fuels for both production of chemicals and energy generations [1-3]. Waste and particularly agricultural biomass such as wood biomass seems to be a realistic alternative power generation leading to technical, economical and environmental benefits [4]. In the international front, several studies and works [5-8] have shown interesting results in the use of wood waste to generate products with higher sell and market valuation. There are examples in the field of composite materials (cellulose nanofibers), biofuels (bio-fuels, char and gaseous products), fertilizers and composting, and among others [9, 10].

There are several alternative and disposal methods used to investigate the minimization of the wastes and various lignocellulosic biomasses [11]. Among these methods, we have thermochemical conversion process which presents several environmental advantages such as the reduction in mass and volume of disposed solids, the reduction in pollutants and the potential for energy recovery [12-14]. Thermochemical conversion such as pyrolysis could be a viable option for environmentally acceptable way to manage waste wood biomass such as sawdust wood (SW) waste, and to manage agricultural biomasse wastes in general [1, 15]. Three products are obtained from pyrolysis; bio-oil (condensable volatiles), bio-char (carbonaceous residue) and bio-gas products (non-condensable) [2, 16]. The first product (bio-oil) can be modified to an alternative energy source, or it may be utilized as raw material for petrochemical production. The second product (bio-char) has potential to be applied into the soil for improving N fertilizer use efficiency or can be used as an adsorbent, while for the third product (bio-gas), it could be used as an alternative energy source or to supply heat for driving the pyrolysis process [4, 17-19].

To carry out a correct design of the systems for thermochemical treatment and control them properly, it's important to know the different states and complex transitions that take place in the waste wood biomass as the temperature varies [20]. The knowledge of the reactivity and the pyrolysis kinetics of the waste biomass give valuable information for the pyrolysis system of the biomass [21]. TGA, named thermogravimetric analysis is one of the main and common method and techniques used for the study of the thermal behavior of lignocellulosic biomass (contain; cellulose, hemicellulose, and lignin) and the kinetics of the thermal decomposition reactions of different solid fuels [22].

Thermogravimetric analysis (TGA) provides a measurement of the mass loss of the sample waste as a function of temperature and time [8-23]. Thermogravimetric is normally performed in either a non-isothermal or isothermal mode. Evaluating the reaction kinetics by a non-isothermal is advantageous in that considerably fewer experimental data are required than in the isothermal method, and the kinetics can be probed over the entire temperature range in a continuous manner [24-26].

In this work, advanced thermochemical conversion technologies are used to study the thermal degradation of waste wood such as sawdust waste wood sample. TG has been used to evaluate the thermal behavior in inert atmosphere of sawdust wood (SW) waste. The calculation of apparent activation energies E_a , order (n), and function of degradation $f(x)$ were based on the application of the isoconversional and model-free methods of Friedman, Vyazovkin, Kissinger-Akahira-Sunou, Flynn-Wall-Ozawa, Starink, Avrami theory, Coats-Redfern and Criado methods. This research has been conducted as a contribution to the development of advanced thermochemical processes such as pyrolysis.

2. Experimental

2.1. Materials and samples preparation

The sawdust wood wastes samples were obtained from Beni-Mellal area (central zone) which located about 304 Km of Rabat and 192 Km of Marrakech (Morocco). These samples were obtained from the carpentry of construction in the middle of the city. The samples were air-dried and ground to obtain a uniform material of average particle size (0.1-0.15 mm). The chemical compositions and the main characteristics of sawdust wood samples are depicted in Table 1.

Table1:Main characteristic of sawdust wood waste (SW)

	Sawdust wood (Wt%)
Proximate Analysis	
Moisture	6.02
Volatile Matter	75.16
Ash	11.95
Fixed Carbon ^(a)	6.87
Chemical Analysis	
Hemicellulose	26.7
Cellulose	40.1
Lignin	33.2
Elemental Analysis	
C	46.01
H	6.92
N	1.20
S	0.81
O ^(a)	45.06
O/C molar proportion^(b)	0.73
H/C molar proportion^(b)	1.80
Empirical formula	CH _{1.800} O _{0.730} N _{0.022}
(a): By difference; (b): Calculated	

2.2. Experimental techniques

SW wastes samples were subjected to TG in an inert atmosphere of nitrogen. *Rheometric Scientific STA 1500* TGA analyzer was used to measure and record the sample mass change with temperature over the course of the pyrolysis reaction. Thermogravimetric curves were obtained at four different heating rates (2, 5, 10 and 15 °C/min) between 20 and 950 °C. Nitrogen gas was used as an inert purge gas to displace air in the pyrolysis zone, thus avoiding unwanted oxidation of the sample. A flow rate of around 60 mL.min⁻¹ was fed to the system from a

point below the sample and a purge time of 60 min (to be sure the air was eliminated from the system and the atmosphere is inert). The balance can hold a maximum of 45 mg, therefore, all samples amounts used in this study averaged approximately 20 mg. The reproducibility of the experiments is acceptable, and the experimental data presented in this paper corresponding to the different operating conditions are the mean values of run carried out three times.

2.3. Kinetic modelling

Kinetic analysis techniques have been classified as either model-fitting (i.e. the identification of a kinetic reaction model) or isoconversional (i.e. model-free) [27]. The latter is preferred by researchers for two reasons; (a) model-free kinetics are sufficiently flexible to allow for a change in mechanism during a reaction, and (b) mass loss transfer limitations are reduced by the use of multiple heating rates. In contrast, model-fitting kinetic methods generally involve a single heating rate, which is disadvantageous because the activation energy varies with the heating rate due to mass/energy transfer effects [28]. The conversion of biomass can be calculated as:

$$x = \frac{m_0 - m_t}{m_0 - m_\infty} \quad (1)$$

Where m_t is the mass of the sample at a given time t and m_0 and m_∞ refer to values at the beginning and the end of the mass loss event of interest.

The rate of heterogeneous solid-state reactions can be generally described by:

$$\frac{dx}{dt} = K(T) \cdot f(x) \quad (2)$$

$K(T)$ is a temperature dependent constant and $f(x)$ is reaction model, which describes the dependence of the reaction rate on the extent of reaction.

The mathematical description of the data for a single-step solid-state decomposition is usually defined in terms of a kinetic triplet [29]: the activation energy, E ; the Arrhenius parameter, A ; and an algebraic expression of the kinetic model as a function of the fractional conversion x , $f(x)$. These terms can be related to experimental data as follows:

$$\frac{dx}{dt} = A_x \cdot \exp\left(\frac{-E}{RT}\right) \cdot f(x) \quad (3)$$

2.3.1. Friedman method (FR) [30]

This method is a differential isoconversional method, and it directly based on Eq. (3) whose logarithm is:

$$\ln\left(\frac{dx}{dt}\right) = \ln(f(x) \cdot A_x) - \frac{E}{RT_x} \quad (4)$$

For this equation, it's easy to obtain values for E over a wide range of conversion by plotting $\ln(dx/dt)$ against $1/T$ for a constant x value.

2.3.2. Flynn-Wall-Ozawa method (OFW) [31-34]

The above rate expression can be transformed into non-isothermal rate expressions describing reaction rates as a function of temperature at a constant β ($\beta=dT/dt$):

$$\frac{dx}{dT} = \frac{A_x}{\beta} \cdot \exp\left(\frac{-E}{RT}\right) \cdot f(x) \quad (5)$$

Integrating up to the conversion, a, Eq. (5) gives

$$\int_0^x \frac{dx}{f(x)} = g(x) = \frac{A_x}{\beta} \int_{T_0}^T \exp\left(\frac{-E_x}{RT}\right) dT \quad (6)$$

Where $g(x)$ is the integral kinetic function or integral reaction model when its form is mathematically defined. One of the methods to obtain the E form dynamic data may be the one used by Flynn, Wall and Ozawa using the Doyle's approximation of $p(x)$, which involves measuring the temperatures corresponding to fixed values of x from experiments at different heating rates. This is one of the integral methods that can determine the E which does not require the knowledge of reaction order.

$$\ln(\beta) = \ln\left(\frac{AE}{Rg(x)}\right) - 5.331 - 1.052\frac{E}{RT_x} \quad (7)$$

Thus, for $x = \text{const.}$, the plot $\ln \beta$ versus $1/T$, obtained from curves recorded at several heating rates, should be a straight line whose slope can be used to evaluate the activation energy.

2.3.3. Vyazovkin method (VYA) [35]

Another isoconversional method is the one developed by Vyazovkin and Lesnikovick that allows both simple and complex reactions to be evaluated.

In Eq. (6), since $E/2RT \gg 1$, the temperature integral can be approximated by:

$$\int_{T_0}^T \exp\left(\frac{-E_x}{RT}\right) dT \approx \frac{R}{E} T^2 \exp\left(\frac{-E_x}{RT}\right) \quad (8)$$

Substituting the temperature integral and taking the logarithm, we have that:

$$\ln\left(\frac{\beta}{T^2}\right) = \ln\left(\frac{RA_x}{Eg(x)}\right) - \frac{E}{RT_x} \quad (9)$$

For each conversion value (x), $\ln(\beta/T^2)$ plotted versus $1/T$ gives a straight line with slope $-E/R$, thus, E is obtained as a function of the conversion.

2.3.4. Kissinger-Akahira-Sunose method (KAS) [36, 37]

The standard Eq. (5) can be written, as follows:

$$\frac{dx}{dT} = \frac{A_x}{\beta} \cdot \exp\left(\frac{-E}{RT_m}\right) \cdot f(x) \quad (10)$$

Which is integrated with the initial condition of $x=0$ and $T=T_0$ to obtain the following expression:

$$\int_0^x \frac{dx}{f(x)} = g(x) = \frac{A_x}{\beta} \int_{T_0}^T \exp\left(\frac{-E_x}{RT_m}\right) \cong \frac{E_x A_x}{\beta R} p\left(\frac{E_x}{RT_m}\right) \quad (11)$$

Essentially the technique assumes that the A , $f(x)$ and E are independent of T while A , $f(x)$ and E are independent of x , then Eq. (11) may be integrated to give the following equation in logarithmic form:

$$\ln g(x) = \ln\left(\frac{E_x A_x}{R}\right) - \ln \beta + \ln p\left(\frac{-E}{RT_m}\right) \quad (12)$$

The KAS method is based on the Coats-Redfern approximation according to which:

$$p\left(\frac{E_x}{RT_m}\right) \cong \frac{\exp\left(\frac{-E_x}{RT_m}\right)}{\left(\frac{E_x}{RT_m}\right)} \quad (13)$$

From relationships (11) and (13) it follows that:

$$\ln \frac{\beta}{T_m^2} = \ln\left(\frac{RA_x}{g(x) \cdot E_x}\right) - \frac{E_x}{RT} \quad (14)$$

2.3.5. Starink method (ST) [38, 39]

According to the Starink method, the approximate expression of OFW method and KAS method can be transformed into the same general formula as:

$$\ln \frac{\beta}{T^s} = C_s - \left(\frac{BE_x}{RT} \right) \quad (15)$$

Where for FWO method; $s=0, B=0.4567$; for the KAS method; $s=2, B=1$. After a further exact analysis by Starink, the parameters of s and B has been adjusted to $s=1.8, B=1.0033$, respectively. Besides, it has been verified by Starink that the precision of apparent activation energy calculated by this method is higher than those of FWO and KAS methods. Hence the Starink method can be described as:

$$\ln \left(\frac{\beta}{T^{1.8}} \right) = C_s - 1.0037 \left(\frac{E_x}{RT} \right) \quad (16)$$

For a given conversion degree x , the points of $\ln(\beta/T^{1.8})$ versus $1/T$ at different temperature heating rates can be fitted to a straight line, and the slope of the line corresponds to $-1.0037E_x/R$. Hence the apparent activation energy E_x can be calculated from the slope of the straight line.

2.3.6. Avrami theory (AT) [40, 41]

Reaction order is also a significant parameter to investigate the pyrolysis characteristic of biomass, besides apparent activation energy. In order to calculate the reaction order. Avrami theory was used in this study, and it can be described as:

$$x = 1 - \exp\left(\frac{-K(T)}{\beta^n}\right) \quad (17) \quad \text{with} \quad K(T) = A_x \exp\left(\frac{-E_x}{RT_x}\right)$$

Where, n represents the reaction order. Taking the double logarithm and transporting. Eq. (17) is transformed into the following equation:

$$\ln(-\ln(1-x)) = \ln A_x - \frac{E_x}{RT_x} - n \ln \beta \quad (18)$$

For a given temperature, T , the points of $\ln(-\ln(1-x))$ versus $\ln \beta$ at different heating rates can be fitted to a straight line, and the slope of the line corresponds to $-n$. Thus, the reaction order can be deduced from the slope of the straight line.

2.3.7. Coats-Redfern method (CR) [42, 43]

Coats-Redfern method is also an integral method, and it involves the thermal degradation mechanism. Using an asymptomatic approximation for resolution of Eq. (11), ($2RT/E \ll 1$) the following equation can be obtained:

$$\ln \frac{g(x)}{T^2} = \ln \left(\frac{A_x R}{\beta E_x} \right) - \frac{E_x}{RT_x} \quad (19)$$

2.3.8. Criado method (Cri) [44]

If the value of the activation energy is known, the kinetic model of the process can be determined by this method. Combining the Eq. (10) with Eq. (19), the following equation is obtained:

$$\frac{Z(x)}{Z(0.5)} = \frac{f(x).g(x)}{f(0.5).g(0.5)} = \left(\frac{T_x}{T_{0.5}} \right)^2 \frac{(dx/dt)_x}{(dx/dt)_{0.5}} \quad (20)$$

Where 0.5 refers to the conversion in $x=0.5$

The left side of Eq. (20); $f(x).g(x)/f(0.5).g(0.5)$ is a reduced theoretical curve, which is characteristic of each reaction mechanism, whereas the right side of the equation associated with the reduced rate can be obtained from experimental data. A comparison of both sides of Eq. (20) tells us which kinetic model describes an experimental reactive process. Table 2, indicates the algebraic expressions of $f(x)$ and $g(x)$ for kinetic models used.

Table2: Algebraic expression of functions of the most common reaction mechanisms

Mechanism		$f(x)$	$g(x)$
Avrami-Erofe'Ve A_n	Avrami-Erofe'Ve- A_2	$2(1-x)[-ln(1-x)]^{1/2}$	$[-ln(1-x)]^{1/2}$
	Avrami-Erofe'Ve- A_3	$3(1-x)[-ln(1-x)]^{2/3}$	$[-ln(1-x)]^{1/3}$
	Avrami-Erofe'Ve- A_4	$4(1-x)[-ln(1-x)]^{3/4}$	$[-ln(1-x)]^{1/4}$
Diffusion D_n	One dimensional diffusion- D_1	$1/2x^{-1}$	x^2
	Two dimensional diffusion- D_2	$[-ln(1-x)]^{-1}$	$[(1-x)ln(1-x)]+x$
	Three dimensional diffusion. Jander- D_3	$3/2(1-x)^{2/3}[1-(1-x)^{1/3}]^{-1}$	$[1-(1-x)^{1/3}]^2$
	Ginstling-Brounshtein- D_4	$3/2[(1-x)-1/3-1]$	$1-(2x/3)-(1-x)^{2/3}$
Reaction order F_n	First-Order-1- F_1	$(1-x)$	$-ln(1-x)$
	Second-Order-2- F_2	$(1-x)^2$	$(1-x)^{-1}-1$
	Third-Order-3- F_3	$(1-x)^3$	$[(1-x)^{-2}-1]/2$
Power law P_n	Power law- P_2	$2x^{1/2}$	$x^{1/2}$
	Power law- P_3	$3x^{2/3}$	$x^{1/3}$
	Power law- P_4	$4x^{3/4}$	$x^{1/4}$
Contraction Reaction R_n	Contraction sphere- R_2	$2(1-x)^{1/2}$	$[1-(1-x)^{1/2}]^2$
	Contraction cylinder- R_3	$3(1-x)^{2/3}$	$[1-(1-x)^{1/3}]^3$

3. Results and discussion

3.1. Thermal degradation of Sawdust wood waste

Pyrolysis profiles under inert atmosphere (mass loss TG and derivative mass loss DTG) of sawdust wood wastes samples are reported in Figs. 1 and 2. It's seen that TG and DTG profiles of SW wastes are similar to those described in the literature [2, 4-7]. In general, thermal decomposition of sawdust wood waste was achieved in three different temperature regimes: drying (step I), main devolatilization (step II) and continuous slight devolatilization (step III) (Fig. 2). Between 120 and 130 °C, the moisture in the sample was evaporated, resulting in mass loss. The mass loss in the first step is approximately 6.42 % for samples wastes. After drying (step I), pyrolytic thermal decomposition reaction took place in the temperature range of about 200-400 °C producing condensable and non-condensable volatile gases (step II). The main devolatilization of the wastes samples starts and finishes at 150 °C and 410 °C, respectively. The mass loss of the main pyrolysis is 59.7 %.

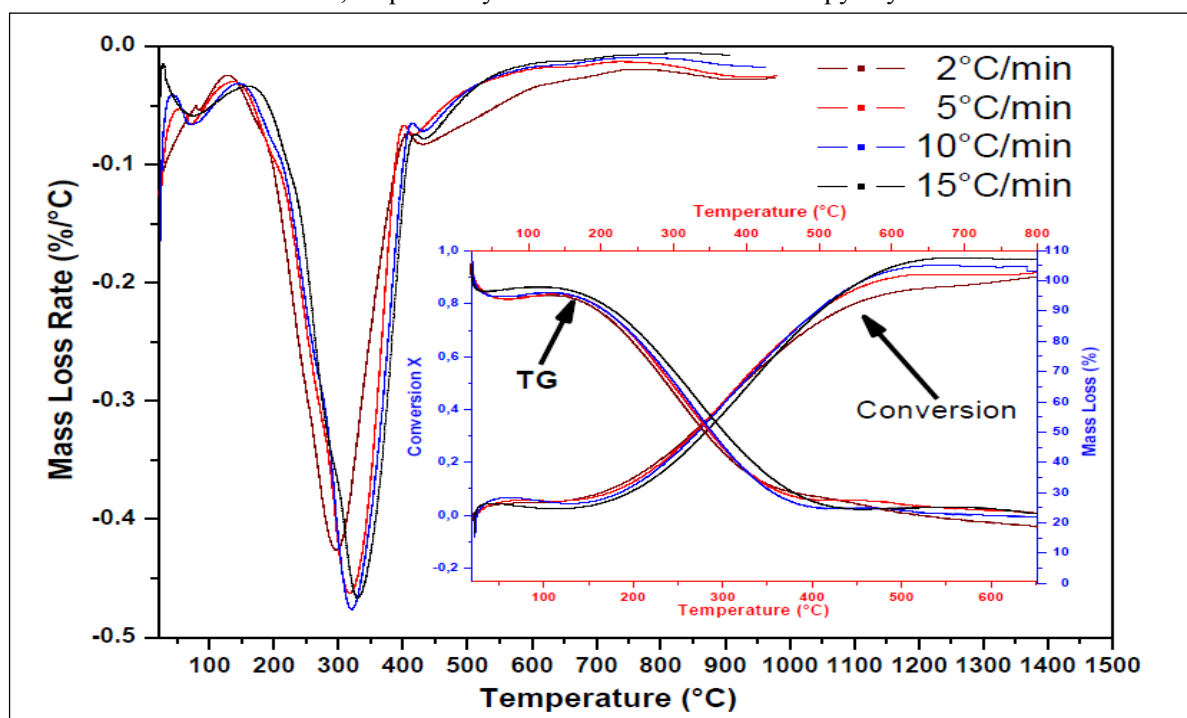


Figure 1:DTG, TG and Conversion curves of Sawdust wood (SW) waste

On the DTG curves, the temperatures at which maximum rate of mass loss occurred are described by the position of the peaks in the curve (Table 3). This step is associated with thermal volatilization of the compounds related to hemicelluloses and cellulose present in the samples wastes. In the case of lignocelluloses material the temperature of degradation and the thermal degradation rate of hemicelluloses and lignin are lower than the values that can be found on the cellulose. After the main pyrolytic process, there is a slow and continuous degradation between 398 °C and 669 °C attributed to lignin degradation (*step III*). A slight mass loss between 650 °C and 850 °C can be assigned to the decomposition of inorganic material. Residual mass at 850 °C is 22.8 % of the initial mass for Sawdust wood sample. With regard to the literature [3, 23] and our study, one can say that the characterization of decomposition of sawdust wood waste sample is in coincidence with the degradation and decomposition rate of other types of wastes and biomasses. But it's differs from point of view, composition, decomposition values, residual masse and temperature of degradation. This due to the composition of samples wastes.

Table 3: Different temperature values of sawdust wood waste

Sample	Heating rate/ °C/min	First Step/°C		Second Step/°C				Third Step/°C	
		T _i	T _f	T _i	T _{max}	T _f	DTG _{max} (%/°C)	T _i	T _f
SW	2	21	150	150	297	398	-0.42702	398	608
	5	23	154	154	314	405	-0.46026	405	650
	10	23	158	158	318	409	-0.47635	409	663
	15	22	164	164	330	410	-0.46279	410	669

Heating rate is one of the most important parameters influencing the pyrolysis characteristics (Figs. 1, 2 and Table 3). It was clear that the heating rate affects significantly the maximum decomposition rate, with maximum decomposition rate tending to increase and occur at higher temperatures when pyrolyzed at higher heating rates (from 2 °C/min to 15 °C/min). The phenomenon related to this important change in the maximum pyrolysis rate can be interpreted by the fact that wood waste such as biomass, has a heterogeneous structure and possesses a number of constituents. These constituents give their characteristic individual decomposition peaks in definite temperature ranges in the pyrolysis process.

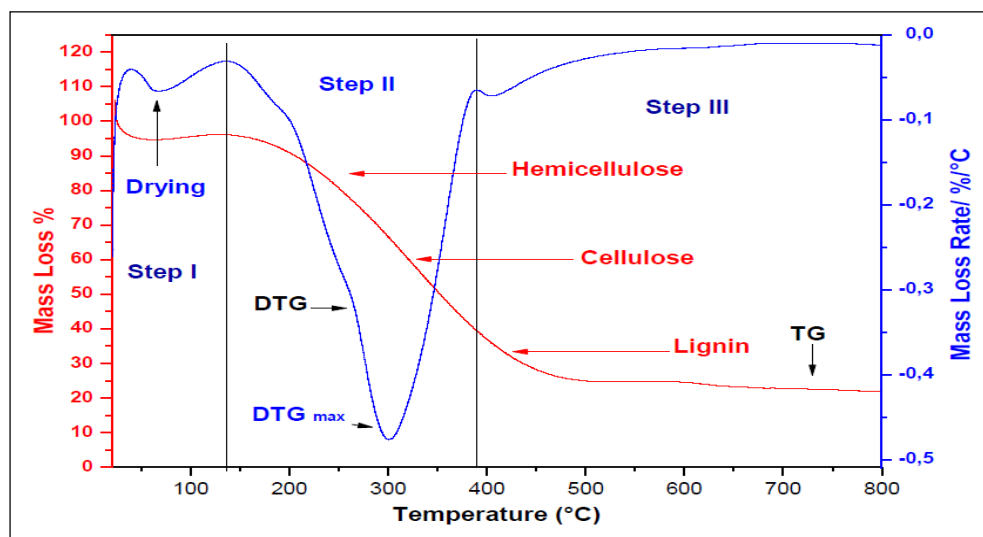


Figure 2: DTG and TG curves of sawdust wood waste at 10 °C/min

When heating rate was sufficiently low during pyrolysis, most of these peaks can be seen as small broken lines or vibrations. However, at high heating rates, separate peaks did not arise because some of them were decomposed simultaneously, and several adjacent peaks were united to form overlapped broader and higher peaks [5,45]. This fact can be a consequence of heat and mass transfer limitations. With an increase in heating rate, the temperature

in the furnace space can be a little higher as the temperature of a particle and the rate of decomposition are higher than the release of volatilities. Because of the heat transfer limitation, temperature gradients may exist in the particle. Temperature in the core of a particle can be a bit lower than temperature on its surface, and different decomposition processes or releasing rates can occur. This is the reason why it is necessary to have a small particle, homogenous sample and the heat transfer surface between the sample and the crucible as large as possible [10,15].

3.2. Variation of apparent activation energy of SW

To evaluate the variation of the activation energy on the conversion degree during the major pyrolysis process, thirteen levels of conversion degree x varying from 20 to 80 % with an increment of 5 % employed at different heating rates 2, 5, 10 and 15 °C/min. The change of the conversion x depending on the temperature and heating rates is shown in Fig. 3. The variation of the activation energy as a function of the degree of conversion was studied by the methods using Friedman (FR), Flynn-Wall-Ozawa (FWO), Vyazovkin (VYA), Kissinger-Akahira-Sunose (KAS) and Starink (ST) equations. Linear regression (Fig. 4) was used to obtain the values of activation energies in terms of x in the range of (0.2 - 0.8) or (20 % - 80 %) with an increment of 5 % (Fig. 3).

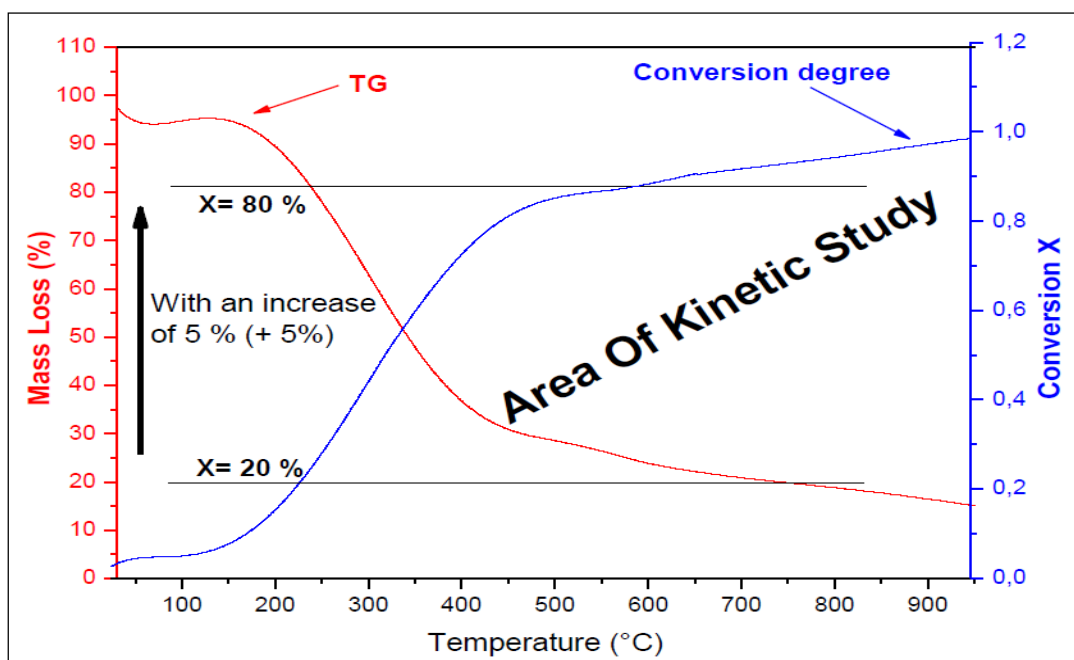


Figure 3: TG and Conversion degree curves of sawdust wood waste at 10 °C/min

The apparent activation energies were obtained from the slope from the intercept of regression lines are given in Table 4. For all the sets of x values, the linear plots of FR, FWO, VYA, KAS and ST methods result in a correlation coefficient (R^2) higher than 0.980. The dependence of apparent activation energy (E_x) on the degree of conversion (x) for decomposition process of sawdust wood obtained by isoconversional methods is presented in Fig. 5.

It can be seen from Table 4, which the apparent activation energy of SW samples varied greatly with different conversion degree. The mean values of activation energy obtained from this study were 168.34 KJ/mol for Friedman method, 153.35 KJ/mol for Vyazovkin method, 164.84 KJ/mol for OFW method, 158.55 KJ/mol for KAS method, and 156.47 KJ/mol for Starink method. Activation energy is an obstacle that must be overcome before a chemical reaction is generated and higher value of activation energy means more difficult of a reaction occurs. It determines the reactivity and sensitivity of a reaction rate. So different activation energies at different degree conversions illustrate the multistage characteristic of the thermal decomposition process of Sawdust wood (SW) waste. It also shows the complexity of this physical and chemical transformation, and it should contain different reactions at different reaction stages.

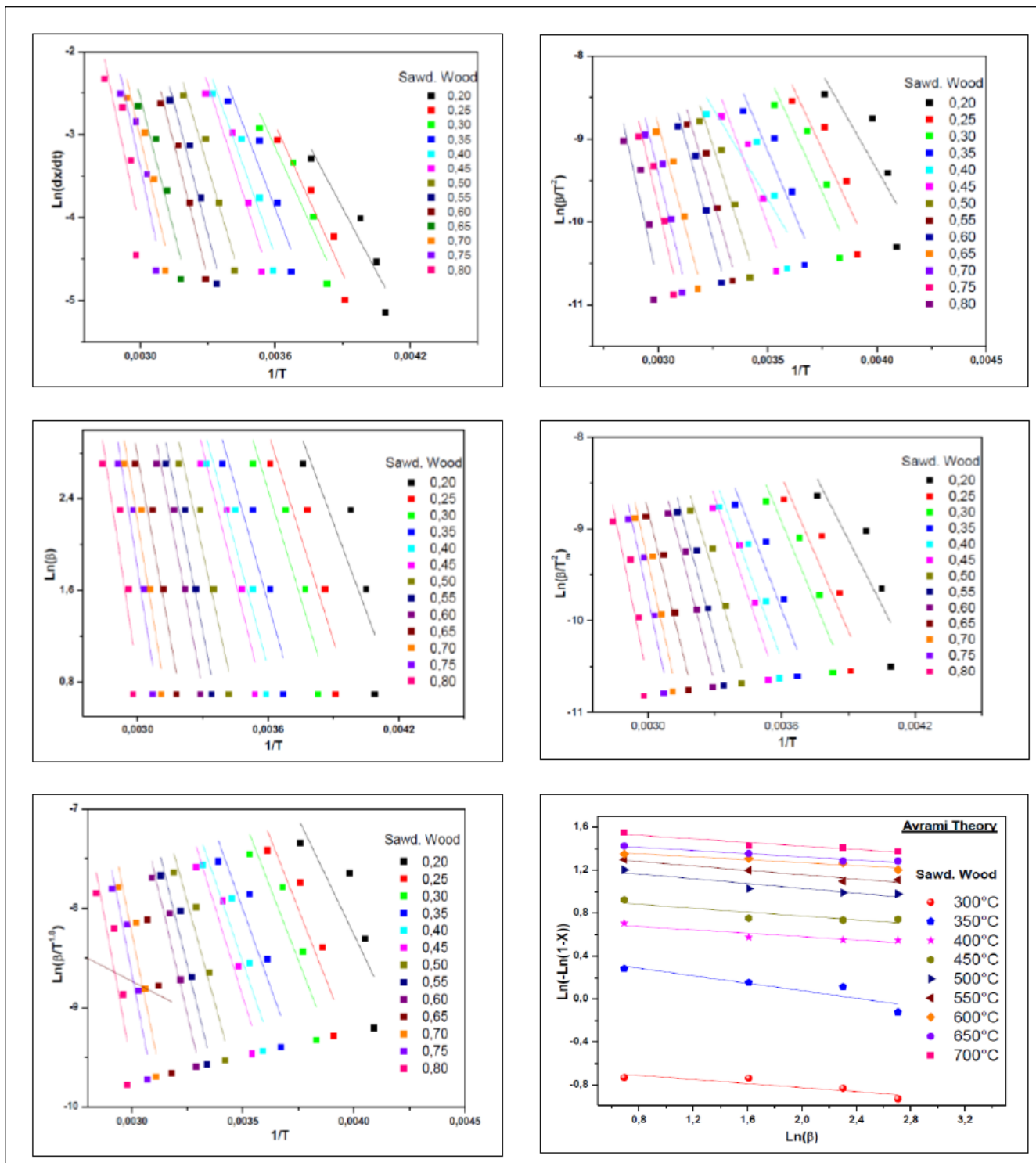
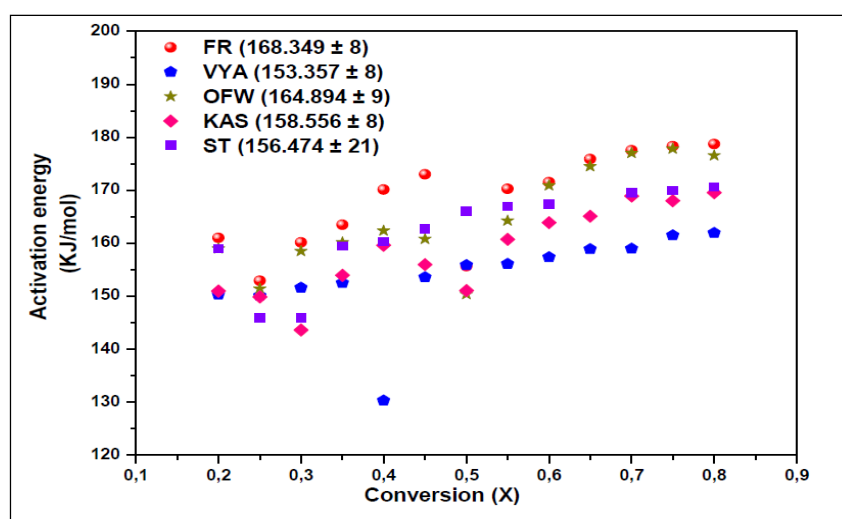


Figure 4:Regression lines to apparent activation energy proposed by FR, VYA, OFW, KAS, ST methods and Avrami theory

From Fig. 5, one can notice the same shapes of the curves E versus x corresponding to the considered methods (FR, FWO, VYA, KAS and ST). This result indicates that the existence of one-step that occurs in cellulose and hemicelluloses decomposition of sawdust wood waste samples. It can be seen that the values of apparent activation energy E calculated by KAS and VYA methods are lower than values of E calculated by FR, FWO and ST methods. Except FR method, all other methods give similar values of E in x degree. The values achieved by FR method were larger than those obtained by FWO, VYA, KAS and ST methods. The difference in calculated E values can also be caused due to the error of improper integration in FWO, VYA, KAS and ST equations. FR method uses instantaneous rate values and so very sensitive to the experimental noises.

Table 4: Activation energy deduced from the FR, VYA, FWO, KAS and Starink methods

Sample	Conversion X	Activation energy (E_x) (KJ/mol)				
		Friedman method (FR)	Vyazovkin method (VYA)	Ozawa-flynn-wall method (OFW)	KAS method (KAS)	Starink method (ST)
SW	0.2	161	150.31	159	151	159
	0.25	152.91	150.1	151.42	149.85	145.91
	0.3	160.16	151.63	158.51	143.61	145.9
	0.35	163.5	152.5	160.17	153.95	159.5
	0.4	170.13	130.32	162.35	159.6	160.33
	0.45	173	153.6	160.80	155.98	162.67
	0.5	155.65	155.9	150.36	151.1	166
	0.55	170.26	156.1	164.23	160.72	166.97
	0.6	171.52	157.36	170.91	163.9	167.41
	0.65	175.87	158.9	174.5	165.1	90.38
	0.7	177.54	159	177	168.9	169.5
	0.75	178.30	161.5	177.83	168	169.97
0.8	178.7	161.97	176.55	169.53	170.63	
Mean		168.349 ± 8	153.357 ± 8	164.894 ± 9	158.556 ± 8	156.474 ± 21

**Figure 5:** Dependence of activation energy on the conversion degree x for decomposition of sawdust waste

3.3. Variation of reaction order and mechanism of SW

During the major pyrolysis process, in order to evaluate the dependence of reaction order on temperature, nine levels of temperature (from 300 °C to 700 °C) were also employed at four temperature heating rates of 2, 5, 10 and 15 °C/min. Adopting the Avrami theory, the regression lines of sawdust wood waste are shown in Figure 4. And the calculated reaction order is listed in Table 5. The corresponding values of R^2 are presented in Table 5. It can be seen from Table that the Avrami theory is suitable for determining the kinetic parameter of reaction order, based on the data of R^2 calculated. The reaction order of sawdust wood differed greatly rather than remained constant. With varied temperatures (300 – 700 °C), the reaction order of sawdust was first increased from 0.1072 to 0.2587 and then decreased to 0.1635.

A model or kinetic method is a mathematical, theoretical description of what occurs experimentally [42, 45]. In solid state reactions, a model can illustrate a particular reaction type and interpret that mathematically into a rate equation. Many methods and models have been proposed in solid-state kinetics, and these methods have been developed based on certain mechanistic assumptions [42]. Other methods are more empirically based, and their mathematics facilitates data analysis with little mechanistic meaning. Therefore, different rate expressions are produced from these models [43, 46].

Table 5: Slope, reaction order (n) and correlation coefficient (R^2) deduced from Avrami theory of SW waste

Sample	Temperature (°C)	Slope	n	R ²
SW	300	-0.1072	0.1072	0.992
	350	-0.1460	0.146	0.90
	400	0.1579	0.1579	0.986
	450	-0.208	0.2080	0.966
	500	-0.2587	0.2587	0.95
	550	-0.2432	0.2432	0.997
	600	-0.2023	0.2023	0.952
	650	-0.1878	0.1878	0.94
	700	-0.1635	0.1635	0.901

In order to find the kinetic model of thermal degradation of SW wastes samples, the Coats-Redfern and Criado methods were chosen as they involve the degradation mechanisms. To determine the most probable model, Coats-Redfern method was used, activation energy for every $g(x)$ function listed in table 2 can be calculated at 10 °C/min, from fitting $\ln(g(x)/T^2)$ versus $1/T$ plots (Figure 6). The activation energies and coefficient correlations at 10 °C/min are tabulated in table 6. To obtain the degradation mechanism of sawdust sample, we have compared the activation energies obtained by the models above, it could be found that the E values of sawdust wood waste corresponding to mechanisms F_1 (160 KJ/mol) is in agreement with the mean values obtained by Friedman, Flynn-wall-ozawa, Vyazovkin, Kissinger and Starink methods (153-168 KJ/mol) (Figure 7).

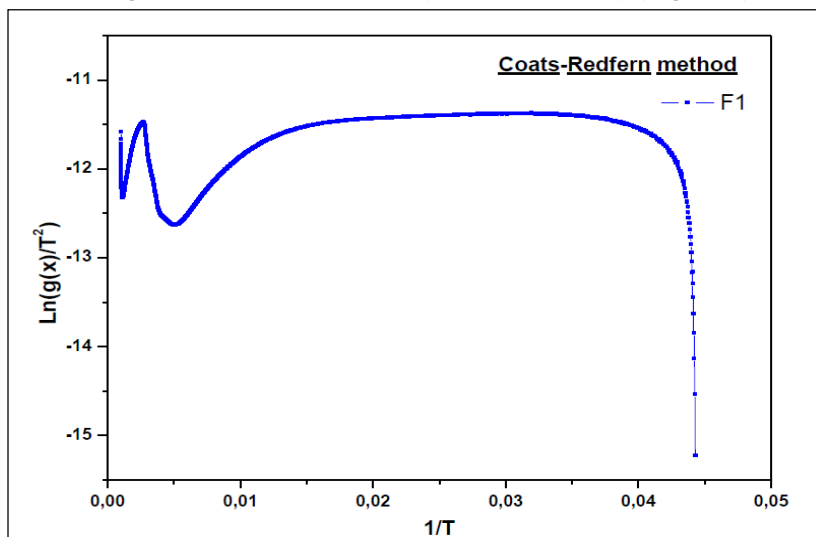
**Figure 6:** Plot of $\ln(g(x)/T^2)$ versus $1/T$ for F_1 model for SW thermal degradation

Fig 6 shows the plot of $\ln(g(x)/T^2)$ versus $1/T$ for F_1 model. With correlation coefficient greater than 0.90 (> 0.9). According to Coats-Redfern equation, if a correct model is selected for the reaction, the plot of $\ln(g(x)/T^2)$ versus $1/T$ will be linear as possible with high-correlation coefficient. One can say that the Coats-Redfern method reliability is not enough and cannot be used to kinetics assessment of reactions. From this point of view the use of the method of Criado is very important, this method gives us more information and can be additional to Coats-Redfern method. The used models and the expressions of associated functions $f(x)$ and $g(x)$ are shown in table 2. The master curve plots $Z(X)/Z(0.5)$ versus x for different mechanisms according to the Criado method for sawdust wood waste sample is illustrated in Fig 7. As can be seen, the comparison of the experimental master plots with theoretical, ones revealed that the kinetic process for the degradation of sawdust sample was most probably described by the reaction order F_1 (F_n model). Concerning reaction order, order-based models (F_n) are the simplest models as they are similar to those used in homogeneous kinetics. In these models, the reaction rate is proportional to concentration, amount or fraction remaining of reactant raised to a particular power which is the reaction order.

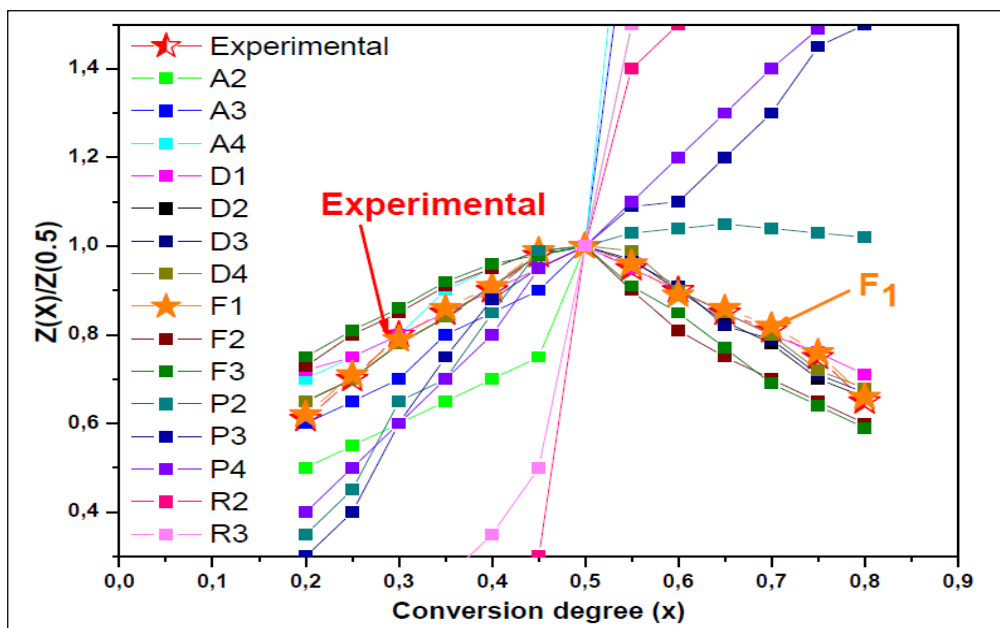


Figure 7: Masterplots of different kinetic models and experimental data at 10°C/min for SW thermal degradation.

Table 6: Activation energy of SW waste degradation obtained by Coats-Redfern method

Model	Activation energy (KJ/mol)	Coefficient R ²
A2	124	0.993
A3	143	0.941
A4	95	0.831
D1	174	0.995
D2	180	0.991
D3	204	0.990
D4	186	0.901
F1	160	0.991
F2	186	0.905
F3	196	0.907
P2	86	0.456
P3	92	0.569
P4	49	0.704
R2	142	0.932
R3	145	0.900

Conclusion

The present study shows that under non-isothermal conditions, in which the sawdust wood waste sample, was heated at four different constant heating rates of 2, 5, 10 and 15 °C/min. With the increase in heating rate, the decomposition process is shifted to a higher temperature zone, but not very distinctly. Eight methods were used for the determination of kinetic reaction parameters: Friedman (FR), Ozawa– Flynn–Wall (FWO), Vyazovkin (VYA), Kissinger-Akahira-Sunose (KAS), Starink (ST), Avrami theory (AT), Coats-Redfern (CR) and Criado (Cri) methods. The values of activation energy of the SW wood waste vary in different thermal degradation temperature ranges. The results showed that apparent activation energy obtained for the decomposition was given as mean values; 168 KJ/mol, 153 KJ/mol and 164 KJ/mol for FR, OFW and VYA methods respectively. While for KAS and ST methods were 158 KJ/mol and 156 KJ/mol. The corresponding values of reaction order (n) was increased from 0.1072 to 0.2587, along with a decrease to 0.1635, and the pyrolysis reaction models of SW sample is described by reaction order F_n , First-order (F_1).

Acknowledgments - The authors would like to thank Prof. Mr. A. Hannioui, Professor of Education, member of Educational Committee of Department of Chemistry and Environment, Faculty of Sciences and Technique, University of Sultan Moulay Slimane, for his invaluable assistance in this work from a financial and material point of view.

References

1. A. Harjanne, J.M. Kohronen. Abandoning the concept of renewable energy. *Energy policy*, 127 (2019) 330-340
2. E.E. Kwon, S. Kim, J. Lee. Pyrolysis of waste feedstocks in CO₂ for effective energy recovery and waste treatment. *Journal of CO₂ utilization*, 31 (2019) 173-180.
3. M. Luisa N.M. Carneiro, M. S.P. Gomes. Energy, Exergy environmental and economic analysis of hybrid waste-to-energy plants. *Energy conversion and management*, 179 (2019) 397-417.
4. V.N. Emel'yanenko, E. Altuntepe, C. Held, A. A. Pimerzin, S.P. Ververkin. Renewable platform chemicals: thermochemical study of levulinic acid esters. *Thermochemica acta*, 659 (2018) 213-221.
5. S. Stakiotakis, D. Vamvuka. Study of co-pyrolysis of olive kernel with waste biomass using TGA/DTG/MS. *Thermochemica acta*, 670 (2018) 44-54.
6. J. Reina, E. Velo, L. Puiyjaner. Thermogravimetric study of the pyrolysis of waste wood. *Thermochemica acta*, 320 (1998) 161-167.
7. Y. Ting Tang, XQ. Ma, Z. Zwang, Z. Wu, Q. Yu. A study of the thermal degradation of six typical municipal waste components in CO₂ and N₂ atmospheres using TGA-FTIR. *Thermochemica acta*, 657 (2017) 12-19.
8. J. A. Conesa, A. Domene. Biomass pyrolysis and combustion kinetics through n-th order parallel reactions. *Thermochemica acta*, 523 (2011) 176-181.
9. F. Yang, A. Zhou, W. Zhao, H. Li. Thermochemical behaviors, kinetics and gas emissions analyses during co-pyrolysis of walnut shell and coal. *Thermochemica acta*, 673 (2019) 26-33.
10. M. G. Sebay Bernd, S.R. Bragança, N. Heck, L.C.P. Dasilv filho. Synthesis of carbon nanostructures by the pyrolysis of wood sawdust in a tubular reactor. *Journal of Materials research and technology*, 6 (2017) 171-177.
11. M. Y. Guida, H. Bouaik, A. Tabal, A. Hannioui, A. Solhy, A. Barakat, A. Aboulkas, K. Elharfi. Thermochemical treatment of olive mill solid waste and olive mill wastewater. *Journal Thermal. Anal and colori*, 123 (2016) 1657-1666
12. A. Margeriat, A. Bouzegane, C. Lorentz, D. Laurenti, N. Guilhaume, C. Mirodatos, C. Geantest, Y. Schuurman. Catalytic conversion of beech wood pyrolytic vapors. *Journal of anal and applied pyrolysis*, 130 (2018) 149-158.
13. G.F. David, O.R. Justo, V.H. Perez, M. Garcia-Perez. Thermochemical conversion of sugarcane bagasse by fast pyrolysis: High yield of levoglucosan production. *J anal and Applied pyrolysis*, 133 (2018) 246-253.
14. J. Zhang, X. Zhang. The thermochemical conversion of biomass into bio-fuels. *Biomass, Biopoly Based materials, and bioenergy*, 2019, 327-368.
15. T.I. Shahan, H. E. Emam. Sono-chemical synthesis of cellulose nanocrystals from wood sawdust using acid hydrolysis. *Internat Journal of bio-macromolecules*, 107 (2018) 5599-1606.
16. H. Gil, A. Ortega, I. Pérez. Mechanical behavior of mortan reinforced with sawdust waste. *Procedia Engineering*, 200 (2017) 325-332.
17. T. Khan. V. Strezov, T.J. Evans. Lignocellulosic biomass pyrolysis: A review of product properties and effects of pyrolysis parameters. *Renewable and Sustain Energy reviews*, 57 (2016) 1126-1140.
18. M.Y. Guida, A. Hannioui. A review on thermochemical treatment of biomass: Pyrolysis of olive mill wastes in comparison with other types of biomass. *Progress in agricultural engineering sciences*, 12 (2016) 1-23.
19. L. Basile, A. Tugnoli, C. Stramigioli, V. Cozzani. Thermal effects during biomass pyrolysis. *Thermochemica acta*, 636 (2016) 63-70.
20. G. Gauthier, T. Melkior, M. Grateau, S. Thiery, S. Salvador. Pyrolysis of centimeter scale wood particles: New experimentl development and results. *J. Anal and Apllied Pyrolysis*, 104 (2013) 521-530.
21. N. Zobel, A. Anca-couce. Slow pyrolysis of wood particles: characterization of volatiles by laser-induced fluorescence. *Proceed of the combys institute*, 34 (2013) 2355-2362.
22. X. Gu, X. Ma, L. Li, C. Liu, K. Cheng, Z. Li. Pyrolysis of poplar wood sawdust by TG-FTIR and PY-GC/MS. *Journal of anal and appli pyrolysis*, 102 (2013) 16-23.
23. E. Grieco, G. Baldi. Analysis and modeling of wood pyrolysis. *Chem. Eng. Science*, 66 (2011) 650-660.
24. G. Mishra, J. Kumar, T. Bhaskar. Kinetic studies on the pyrolysis of pinewood. *Biores Technology*, 182 (2015) 282-288.

25. M. A. Diitenberg, L. E. Hasburgh. Wood products: thermal degradation and fire. Ref Modu in Matrials science and Material engineering. 2016.
26. R. Vi jeu, L. Gerun, M. Tazerout, C. Catelain, J. Bellettre. Dimensional modelling of wood pyrolysis using a nodal approach. *Fuel*, 87 (2008) 3292-3303.
27. M. Y. Guida, H. Bouaik, L. ElMouden, A. Moubarik, A. Aboulkas, K. Elharfi, A. Hannioui. Utilization of starink approach and avrami theory to evaluate the kinetic parameters of the pyrolysis of olive mill solid waste and olive mill wastewater. *J Adv Chem Eng*, 6 (2016) 1-8.
28. L. Mu, J. Chen, H. Yin, X. Song, A. Li. Pyrolysis behaviors and kinetics of refining and chemicals wastewater, lignite and their blends through TGA. *Bioresour Technol*. 2015
29. S. Yaman. Pyrolysis of biomass to produce fuels and chemical feedstocks. *Energy Convers Manag*, 45(2004) 651–671.
30. H.L. Friedman. Kinetics of thermal degradation of char-forming plastics from thermogravimetry. Application to a phenolic plastic. *Journal of Polymer Science Part C: Polymer Symposia*; Wiley Online Library; 1964.
31. J.H. Flynn, L.A. Wall. A quick, direct method for the determination of activation energy from thermogravimetric data. *J Polym Sci, Part C: Polym Lett*, 4(1966) 323–328
32. J.H. Flynn, L.A. Wall. General treatment of the thermogravimetry of polymers. *J Res Nat Bur Stand*, 70 (1966) 487–523.
33. T. Ozawa. A new method of analyzing thermogravimetric data. *Bull Chem Soc Jpn*, 38(1965) 1881–1886.
34. T. Ozawa, Kinetic analysis of derivative curves in thermal analysis, *J Therm Anal Calorim*, 2(1970)301-324
35. S. Vyazovkin, A. Lesnikovick. Transformation of “degree of conversion against temperature” into “degree of conversion against time” kinetic data. *Russ J Phys Chem*, 62(1988) 1525-1570.
36. T. Akahira, T. Sunose. Trans joint convention of four electrical institutes, paper no. 246, 1969 research report. *Chiba institute of technology scien Technol*, 16 (1971) 22-31
37. H.E. Kissinger. Reaction kinetics in differential thermal analysis. *Anal chem.*, 29 (1957) 1702-1706
38. SA. Kumar, P. Gupta, SR. Kumar. Modelling of pyrolysis of large wood particles. *Bioress technolo*, 100 (2009) 3134-3139.
39. M. Y. Guida, A. Hannioui. Evaluation of Reliability of Coats-Redfern and Criado methods for kinetic analysis of olive mill solid waste and olive mill wastewater. *Internatio Journ of Scienti and engineering research*, 11 (2016) 193-203
40. JG. Liu, XM. Jiang, LS. Zhou, XX. Han, ZG. Cui. Pyrolysis treatment of olive sludge and model free kinetics analysis. *J Hazard Mater*, 161 (2009) 1208-1215.
41. AW. Coats, J. Redfern. Kinetic parameters from thermogravimetric data. *Nature*, 201 (1964) 68-9
42. J. Flynn, L.A. Wall. Quick direct method for the determination of activation energy from thermogravimetric data. *Polym Lett*, 4 (1966) 323-8
43. J.M. Criado. Kinetic analysis of DTG data from master curves. *Thermochemica Acta*, 24 (1978) 186-9
44. A. Ammar, R. Douglas. Solid-state kinetic models: basics and mathematical fundamentals. *J. Physi Chem B*, 110 (2006) 17315-17328
45. J.B. Sheldon duff, W. D. Murray. Bioconversion of forest products industry waste cellulotics to fuels ethanol: a review. *Bioress Technolo*, 55 (1996) 1-33.
46. J.J. Morfão, J.L. Figueiredo. A simplified method for determination of lignocellulosic materials pyrolysis kinetics from isothermal thermogravimetric. *Thermochemica acta*, 380 (2001) 67-78.

(2019) ; <http://www.jmaterenvirosci.com>